Journal of Engineering Science and Technology
Vol. 18, No. 2 (2023) 913 - 930

COMPUTATIONAL CALCULATION OF ADSORPTION ISOTHERM CHARACTERISTICS OF CARBON MICROPARTICLES PREPARED FROM MANGO SEED WASTE TO SUPPORT SUSTAINABLE DEVELOPMENT GOALS (SDGS)

ASEP BAYU DANI NANDIYANTO*,
DWI FITRIA AL HUSAENI, RISTI RAGADHITA, MELI FIANDINI,
RINA MARYANTI, DWI NOVIA AL HUSAENI

Universitas Pendidikan Indonesia, Jl. Dr. Setiabudi No. 229 Bandung, Indonesia
*Corresponding Author: nandiyanto@upi.edu

Abstract

This study was conducted to evaluate the adsorption isotherms of carbon microparticles prepared from mango seed waste. Experiments were done by carrying process using several stages: (i) preparing and washing mango seed waste, ii) carbonization of the seeds at a temperature of 230°C for 3 hours, and (iii) grinding of carbonized mango seeds using saw-milling. The batch-reactor technique was used to investigate the adsorption isotherm model using curcumin as the model of dye, in which the adsorption process was done under constant temperature, pressure, and pH conditions. The adsorption results were evaluated using 10 adsorption isotherm models (Langmuir, Temkin, Freundlich, Dubinin-Radushkevich, Hill-Deboer, Jovanovic, Fowler-Guggenheim, Harkin-Jura, Halsey, and Flory-Huggins). These results were in good agreement with some isotherm models, based on the correlation coefficient (R^2), namely Jovanovic (R^2=0.9379), Freundlich (R^2=0.7423), Halsey (R^2=0.7423), and Dubinin-Radushkevich (R^2 = 0.7187), informing that the phenomena during the adsorption were endothermic and spontaneous. The adsorption process interferes monolayer and multilayer formation under molecular-molecular cooperative phenomena. The interactions were confirmed to involve chemisorption and physisorption. This study shows the potential applications of mango seed waste as a sustainable adsorbent source for carbon microparticles and can support sustainable development goals (SDGs).

Keywords: Adsorption, Adsorption isotherm, Carbon, Computational calculation, Mango seed wastes, Microparticle.

1. Introduction

Adsorption is a process of accumulation of many molecules (compounds, ions, or atoms) that occur at the boundary between two phases, namely the interaction between the liquid phase and the liquid phase, the gas phase and the liquid phase, the gas phase, and the solid phase, or the liquid phase and solid phase [1]. Based on the acting force, adsorption is divided into two, namely chemical and physical adsorption [2]. In physical adsorption, the bond strength between the adsorbed molecule and the surface is very weak, while in chemical adsorption the bond plays a very important role and is the result of a transfer or placement of electrons in the reaction between the adsorbent and the adsorbent [3]. The adsorbent material can use from biological materials. Biological adsorbents show the ability of biomass to bind heavy metals through metabolic or chemical-physical steps from a solution and include the removal of toxins from hazardous materials [4]. One of the biological wastes that can be used as an adsorbent is mango seed waste.

Mango seeds are one of the abundant wastes that are disposed of by the mango juice industry and are increasing with the increase in production. Disposal of mango seeds in large quantities directly into the environment can pollute the environment because the nature of mango seeds is easy to rot. Mango seeds contain about 20 - 60% of the weight of the whole fruit. The kernel in the mango seed contains 45-75% of the whole seed weight [5]. The mango seeds' average content consists of carbohydrates (69.22-79.78%), protein (5.6-9.5%), fat (8.35-16, 13%), ash (0.35-3.6%), and fiber (0.14-2.95%) [6]. Mango seeds are also rich in tannins [7].

Tannins contained in plants, one of which is in mango seeds, are an active substance that causes the coagulation process. Meanwhile, natural polymers such as starch function as flocculants [8]. Mango seed extract contains natural polysaccharides consisting of D-galactose, D-glucose, and D-xylose which are natural flocculants. Natural flocculants, especially polysaccharides, are more environmentally friendly when compared to inorganic and organic coagulants [9]. Carbohydrates are organic compounds that belong to the class of polymer compounds. The polymer compound consists of a monomer in the form of D-glucose linked to glucose to form 1,4'-β-D-glucose. Cellulose molecules are entirely linear and have a strong tendency to form intramolecular and intermolecular hydrogen bonds. The bond formed between the hydroxyl groups (-OH) of adjacent glucose units in the cellulose molecule has a large enough potential to be used as an adsorbent. This is because the bonds formed between the hydroxyl groups (-OH) of glucose units can interact with the adsorbate components [10].

There are several previous studies regarding the adsorption process with adsorbent materials from biological waste. There are studies on the use of adsorption in the removal of cadmium from studies using orange waste [11], the adsorption ability in reducing chromium levels in liquid waste using activated carbon of cowhide waste [12], there are studies on the utilization of cocoa pod peel waste as an adsorbent for Rhodammin dye [13], and rice husk as biosorbent [14]. Further previous research is presented in Table 1.

Although many studies have reported the use of waste as an adsorbent, none of these studies has investigated the adsorption isotherm experiment to remove liquid dye from curcumin solution using carbon microparticles from mango seed waste with computational calculation adsorption isotherm models. Therefore, this research is done for an adsorption isotherm experiment using carbon microparticles

of mango seed waste to remove curcumin dye from an aqueous solution. Each calculation of the adsorption isotherm models was carried out using a computational method. By doing this research, more studies can develop and give the added value of waste, especially mango seed waste, for better and more useful products. This study also shows the potential applications of mango seed waste as a sustainable adsorbent source for carbon microparticles and can support sustainable development goals (SDGs), while SDGs is one of the crucial points in many countries [30].

Table 1. Some previous research on the use of agricultural materials in isothermal adsorption.

No.	Absorbent Material	Results	Ref.
1	Palm oil	In comparison to other adsorbents, oil palm has a huge surface area, is simple to source, and is reasonably priced.	[15]
2	Breadfruit	Breadfruit contains cellulose with a level of 17.59% so that it can be used as an adsorbent.	[16]
3	Noni Fruit	Noni juice can improve the quality of used cooking oil and it can be reused as a frying medium.	[17]
4	Sugarcane Dregs	The use of ICP-MS is highly recommended to reduce iron levels in the water.	[18]
5	Salak Seeds	Salak seed biosorbents can adopt chromium dyes and heavy metals.	[19]
6	Rice Husk	The prepared agglomeration carbon particles, having a size of about 800 nm, are efficient to use as adsorbents.	[20]
7	Pumpkin	According to the results, a monolayer of adsorption on the surface of pumpkin carbon microparticles occurred with physical processes.	[21]
8	Pineapple Peel Waste	The results of this study indicate that the adsorption profile with carbon particles from pineapple peel waste as an adsorbent is following the Freundlich model. Interactions between adsorbate molecules and the process of multilayer adsorption on heterogeneous surfaces.	[22]
9	Banana Stem Waste	The adsorption process is included in the monolayer with the type of physical adsorption interaction. Banana stem waste carbon has the potential to be used as an adsorbent.	[23]
10	Rice Straw Waste	This study shows that the use of rice straws is effective for making porous carbon particles and the change in porosity has a direct impact on the product's ability to adsorb molecules.	[24]
11	Silika Particle from Rice Husk	Silica particles from rice husk proved to be effective in the adsorption of curcumin molecules. The adsorption model that is suitable for this research is the Freundlich isotherm model.	[25]
12	Soursop Peel Waste	Particle size effects in predicting the adsorbing process. The adsorption process with soursop peel waste material occurs on the multilayer	[26]

No.	Absorbent Material	Results	Ref.
		surface. The adsorbent-adsorbate interaction is included in physical adsorption.	
13	Red Dragon Fruit Peel Waste	The isotherm model of Dubinin-Radushkevich is the most appropriate adsorption isotherm model with Red Dragon Fruit Peel Waste as the adsorbent.	[27]
14	Calcium Carbonate from Barred Fish (Scomberomorus spp.) Bone	The isotherm model of Dubinin-Radushkevich is the most appropriate adsorption isotherm model. The findings reveal that the multilayer adsorption process occurs for all micrometer sizes and the process is a physical interaction between the adsorbate and the adsorbent surface.	[28]
15	Alang-Alang Plants	Cellulose adsorbent from the alang-alang plant can adsorb methylene blue dye under alkaline conditions of pH 9 with a second-order kinetics rate and tends to be multilayer interaction or the principle of Freundlich adsorption isotherm.	[29]

2. Adsorption Isotherm Models

Figure 1 shows an illustration of the monolayer, multilayer, and cooperative adsorption processes. The adsorption processes depicted in Fig. 1 are phenomena of standard adsorption processes. To assess the phenomena occurring during the adsorption process, ten adsorption isotherm models were utilized, including the Langmuir, Temkin, Freundlich, Flory-Huggins, Dubinin-Radushkevich, Hill-Deboer, Fowler-Guggenheim, Jovanovic, Harkin-Jura, and Halsey models. A more detailed explanation of the adsorption isotherm models is presented in the following [31].

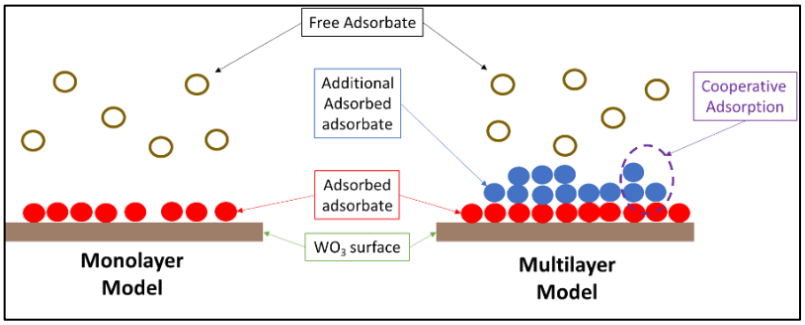

Fig. 1. The monolayer, multilayer, and cooperative adsorption process illustration.

2.1. Langmuir isotherm

Based on the homogeneous single-layer surface adsorption process is the Langmuir isotherm principle. Because no adsorbate transmigrates, the monolayer posits that the molecules adsorbed during the adsorption process do not interact with each other and have the same surface energy. Equations 1 and 2 can be used to predict the Langmuir isotherm equation.

$$\frac{1}{Q_e} = \frac{1}{Q_{max}K_L}\frac{1}{C_e} + \frac{1}{Q_{max}} \quad (1)$$

$$R_L = \frac{1}{1+K_L C_e} \quad (2)$$

where K_L is the Langmuir adsorption constant, Q_{max} is the monolayer adsorption capacity (mg/g), and R_L is the separation factor. Table 2 shows the meaning of the R_L parameter.

Table 2. The R_L parameter meaning.

Condition	Explanation
$R_L > 1$	Unfavourable adsorption because desorption occurs
$R_L = 1$	Linear adsorption process that does not depend on the concentration
$R_L = 0$	Irreversible adsorption process because the adsorbate cannot diffuse (usually occurs in chemisorption)
$0 < R_L < 1$	Favourable adsorption because no desorption occurs

2.2. Freundlich isotherm

Freundlich isotherm based on the adsorption process forming heterogeneous surface layers. Since multilayer adsorption allows interactions between the adsorbed molecules, this model shows the energy at each surface location is different. The Freundlich isotherm model expresses with equation 3.

$$\log Q_e = log k_f + \frac{1}{n}\log C_e \quad (3)$$

where k_f is the Freundlich isotherm model constant that estimates the adsorption capacity, C_e is the adsorbate concentration at equilibrium (mg/L), n is the degree of nonlinearity, and $1/n$ assumes the adsorption strength. Table 3 shows the meaning of n and $1/n$ parameters.

Table 3. The meaning of the n and $1/n$ parameters.

Condition	Explanation
$n < 1$	Characteristic of the adsorption process with the chemisorption process
$n = 1$	Characteristic of a linear adsorption process where there is a partition between two phases that is independent of concentration
$n > 1$	Characteristic of the adsorption process with the physisorption process
$1/n < 1$	Characteristic process of the normal adsorption
$1/n > 1$	Characteristic process of the cooperative adsorption
$1 < 1/n < 0$	Characteristic of a favourable adsorption process because there is no desorption process
$0 < 1/n < 1$	Characteristic of the adsorption process that occurs on heterogeneous surfaces (a $1/n$ value close to 0 indicates that the adsorbent surface is increasingly heterogeneous).

2.3. Temkin isotherm

When using very low adsorbate concentrations, the Temkin isotherm represents the indirect adsorbate interaction. Equation 4 is used to compute the total molecules' adsorption heat in the multilayer.

$$q_e = \beta_T(lnC_e) + (\beta_T lnA_T) \quad (4)$$

where A_T is the equilibrium constant of the Temkin isotherm model and β_T is the Temkin isotherm. β_T parameter is explained in Table 4.

Table 4. The meaning of the β_T parameter.

Condition	Explanation
β_T < 8 kJ/mol	Physical adsorption
β_T > 8 kJ/mol	Chemical adsorption

2.4. Dubinin-Radushkevich isotherm

Adsorption occurs on heterogeneous surfaces, according to the Dubinin-Raduskevich isotherm. Equation 5 depicts the Dubinin-Radushkevich model's adsorption equation.

$$lnq_e = lnq_s - \beta\varepsilon^2 \quad (5)$$

where q_s is the theoretical saturation capacity (mg/g), the average free adsorption energy per mole of adsorbate, which is connected with the Dubinin-Radushkevich isotherm model constant, and ε is the Polanyi potential associated with equilibrium conditions. Equations 6 and 7 expressed the calculation of the Polanyi potential and the adsorption energy.

$$\varepsilon = RT \ln\left[1 + \frac{1}{C_e}\right] \quad (6)$$

$$E = \frac{1}{\sqrt{2\beta}} \quad (7)$$

where E is the adsorption energy which has the meanings shown in Table 5.

Table 5. The meaning of the *E* parameter.

Condition	Explanation
E < 8 kJ/mol	Physical adsorption
E > 8 kJ/mol	Chemical adsorption

2.5. Fowler-Guggenheim isotherm

The isotherm model of Fowler-Guggenheim explains the presence of lateral interactions between adsorbed molecules. Equation 8 expresses the Fowler-Guggenheim isotherm equation.

$$K_{FG}C_e = \frac{\theta}{1-\theta}\exp\left(\frac{2.\theta.W}{RT}\right) \quad (8)$$

where K_{FG} is the Fowler-Guggenheim isotherm equilibrium constant (L/mg), and W is the interaction energy of the adsorbed molecules (kJ/mol). Table 6 summarizes the meaning of the W parameter.

Table 6. The meaning of the *W* parameter.

Condition	Explanation
W > 0 kJ/mol	The attractive force of the adsorbed molecules and the process is exothermic
W < 0 kJ/mol	The repulsion of the process and adsorbed molecule is endothermic.
W = 0 kJ /mol	Adsorbed molecules do not interact

2.6. Hill-de Boer isotherm

With lateral interactions between the molecules that have been adsorbed, the Hill-de Boer isotherm depicts mobile adsorption. The Hill-de Boer isotherm's equation is given by equation 9.

$$K_1.C_e = \frac{\theta}{1-\theta}\exp\left(\frac{\theta}{1-\theta} - \frac{K_2\theta}{RT}\right) \quad (9)$$

where K_1 is the Hill-de Boer constant (L/mg), and K_2 is the adsorbed molecular interaction energetic constant. Table 7 shows the meaning of the K_2 parameter.

Table 7. The meaning of the K_2 parameter.

Condition	Explanation
$K_2 > 0$ kJ/mol	The attractive force between the adsorbed molecules and the process is exothermic
$K_2 < 0$ kJ/mol	The repulsion between the process and the adsorbed molecule is endothermic.
$K_2 = 0$ kJ/mol	Adsorbed molecules do not interact

2.7. Jovanovic isotherm

The Jovanovic isotherm is based on the Langmuir model's phenomena, however, it does not allow for mechanical contact between the adsorbent and the adsorbate. Equation 10 shows the linear equation of the Jovanovic isotherm.

$$lnQ_e = lnQ_{max} - K_jC_e \quad (10)$$

where Q_e is the adsorbate amount in the adsorbent at equilibrium (mg/g), Q_{max} is the maximum absorption of the adsorbate, and K_J is the constant of Jovanovic.

2.8. Harkin-jura isotherm

The Harkin-Jura isotherm analyses adsorption on a heterogeneous surface where a multilayer is formed during the adsorption process. Equation 11 represents the equation of this model.

$$\frac{1}{q_e^2} = \frac{B_{HJ}}{A_{HJ}} - \left(\frac{1}{A}\right) logC_e \quad (11)$$

where B_{HJ} is connected to the adsorbent-specific surface area and A_{HJ} is the Harkin-Jura constant.

2.9. Flory-Huggins isotherm

The Flory-Huggins accounts for the adsorbate's surface blanketing on the adsorbent and assumes that adsorption happens spontaneously. The Flory-Huggins isotherm is represented by Equation 12.

$$log\frac{\theta}{C_e} = logK_{FH} + n\log(1-\theta) \quad (12)$$

where $\theta = (1 - \frac{C_e}{C_o})$ which indicates the surface blanketing degree, K_{FH} is the constant of Flory-Huggins isotherm, and the amount of adsorbate occupying the adsorption location is measured by n_{FH}. Equation 13 is used to compute the adsorption Gibbs free energy (ΔG°) that occurs spontaneously.

$$\Delta G° = -RT\ln K_{FH} \quad (13)$$

the negative value of ΔG° shows the process of adsorption depends on temperature and spontaneous.

2.10. Halsey isotherm

The Halsey is used to measure adsorption with multilayer properties. Equation 14 depicts Halsey isotherm's equation.

$$Q_e = \frac{1}{n_H} lnK_H - \left(\frac{1}{n_H}\right) lnC_e \quad (14)$$

where K_H and n are Halsey's isotherm constants.

Table 8 shows the curves of the data fitting findings as well as the calculations for each adsorption isotherm parameter.

Table 8. Adsorption isotherms fitting data, calculation, and their parameters.

Isotherm Model	Linear Equation	Plotting		Parameters
		x-Axis	y-Axis	
Langmuir	$\frac{1}{Qe} = \frac{1}{QmaxK_L}\frac{1}{Ce} + \frac{1}{Qmax}$	$1/C_e$	$1/Q_e$	• $\frac{1}{Q_{max}} = intercept$ • $K_L = \frac{1}{Q_{max} \times slope}$
Freundlich	$\ln Q_e = \ln k_f + \frac{1}{n}\ln C_e$	lnC_e	lnQ_e	• $lnK_F = intercept$ • $\frac{1}{n} = slope$
Temkin	$q_e = B_T \ln A_T + B_T \ln Ce$	lnC_e	Q_e	• $B = slope$ • $B_T lnA_T = intercept$ • $B_T = \frac{RT}{B}$
Dubinin-Radushkevich	$\ln q_e = \ln q_s - (\beta\varepsilon^2)$	ε^2	lnQ_e	• $\beta = K_{DR} = slope$ • $E = \frac{1}{\sqrt{2 \times K_{DR}}}$
Flory Huggins	$log\frac{\theta}{C_e} = logK_{FH} + n\log(1-\theta)$	$\log\left(\frac{\theta}{C_0}\right)$	$log(1-\theta)$	• $n_{FH} = slope$ • $k_{FH} = intercept$ • $\Delta G^o = RT\ln(k_{FH})$ $\theta = 1 - (\frac{C_e}{C_0})$
Fowler-Guggenheim	$ln\left(\frac{C_e(1-\theta)}{\theta}\right) - \frac{\theta}{1-\theta} = -lnK_{FG} + \frac{2W\theta}{RT}$	θ	$ln\left[\frac{C_e(1-$	• $W = slope$ • $-lnK_{FG} = intercept$ • $\alpha\ (slope) = \frac{2W\theta}{RT}$ $\theta = 1 - (\frac{C_e}{C_0})$

Isotherm Model	Linear Equation	Plotting		Parameters
		x-Axis	y-Axis	
Hill-Deboer	$ln\left[\frac{C_e(1-\theta)}{\theta}\right] - \frac{\theta}{1-\theta} = -lnK_1 - \frac{K_2\theta}{RT}$	θ	$ln\left[\frac{C_e(1-}{\theta}\right] - \frac{\theta}{1-\theta}$	• $-lnk_1 = intercept$ • $\alpha\ (slope) = \frac{k_2\theta}{RT}$ • $\theta = 1 - (\frac{C_e}{C_0})$
Jovanovic	$lnq_e = lnq_{max} - K_J C_e$	C_e	lnQ_e	• $K_J = slope$ • $lnq_{max} = intercept$
Harkin-Jura	$\frac{1}{q_e^2} = \frac{B}{A} - \left(\frac{1}{A}\right) logC_e$	$logC_e$	$\frac{1}{q_e^2}$	• $A_H = \frac{1}{Slope}$ • $\frac{B_H}{A_H} = intercept$
Halsey	$lnQ_e = \frac{1}{n_H} lnK_H - \frac{1}{n} lnC_e$	lnC_e	lnQ_e	• $\frac{1}{n} = slope$ • $\frac{1}{n} lnK_H = intercept$

The adsorbent unit mass at equilibrium (Q_e) is added using Equation 15.

$$Q_e = \frac{C_o - C_e}{m} \times V \quad (15)$$

where C_o is the early concentration (mg/L), C_e is the equilibrium concentration (mg/L), m is the adsorbent mass (g), and V is the adsorbate solution volume (L).

3. Method

3.1. Materials

This study used various materials, namely mango seed waste (Kweni Mango seed), water, and curcumin (which were obtained by extracting turmeric from a local market in Bandung, Indonesia). The turmeric extraction process is described in more detail in research in the literature [32].

3.2. Preparation of calcium carbonate particles from mango seed

Mango seed samples were separated from the flesh. Then, the mango seed samples were washed and carbonized using an oven at 230°C for 10 hours. The carbonized mango seed model was ground using a sawmill for 2 minutes to obtain a homogeneous size. Particles that have been ground are then filtered using a sieve-test (PT Rumah Publication Indonesia), sieve-mesh hole sizes of 500, 250, 100, 74, dan 60 μm to obtain specific sizes. A detailed milling process is reported in our previous studies [33, 34].

3.3. Characterization of particles

The particle size and morphology of the raw material carbon of mango seed waste were investigated using a digital microscope. The chemical characteristics of the mango seed waste carbon were analysed to determine the structural elements of the

product. Chemical characterization analysis was carried out using Infrared Fourier transform (FTIR-6600, FTIR, Jasco Corp., Japan).

3.4. Batch adsorption experimental

The batch experiment was carried out by adding 0.05 g of carbon particles (as adsorbent) to a solution of curcumin with specific concentrations of 100, 80, 60, 40, and 20 ppm with a volume of 140 mL in a beaker glass. The curcumin-carbon solution was mixed quickly throughout the adsorption test, at a speed of 1000 rpm for 120 minutes at ambient conditions with a persistent pH (approximately 7). After that, a sample of the combined solution was obtained and filtered using a nylon membrane syringe filter with a 0.22 m pore size. Then, after the process of adsorption was completed, the solution concentration was analysed using Visible Spectroscopy (Model 7205; Jenway; Cole-Parner; US). The concentration of the solution was analysed with the maximum wavelength being in the range of 280 to 500 nm.

The results of adsorption were then plotted and normalized. Detailed information for calculating isotherm is in our previous study [35]. Beer's law was used to calculate the maximum absorption peak to obtain the curcumin concentration. The data of concentration obtained were plotted and compared with 10 standard adsorption isotherm models, namely the Langmuir, Hill-Deboer, Freundlich, Jovanovic, Temkin, Dubinin-Radushkevich, Fowler-Guggenheim, Flory-Huggins, Harkin-Jura, and Halsey models. The computation of standard adsorption isotherm models is carried out using a computational principle with an excel program.

4. Results and Discussion

4.1. Physical properties of carbon particles

Figures 2(a) and (b) show a digital microscope image respectively and Fig. 2(c) is a carbon particles Ferret analysis prepared from mango seed waste. Figures 2(a) and (b) shows that the carbon particles have an inhomogeneous size. Figure 2(c) shows the distribution of carbon particles with sizes ranging from 100 dan 500 μm. The average particle size of carbon is 240 μm.

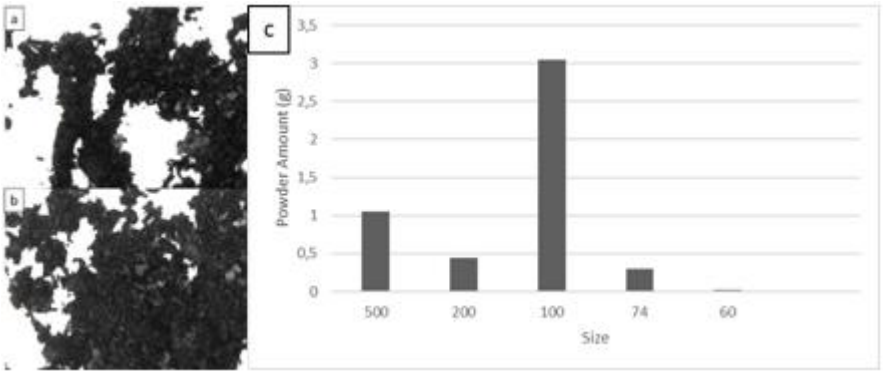

Fig. 2. The digital microscope of particles carbon (a-b) and Ferret analysis of particle size (c).

4.2. Carbon particles adsorption characteristics based on isotherm models

Figure 3 depicts the results of the adsorption process computational calculation plot with the 10 adsorption isotherm models determined at the outset. Based on the results of the data plot procedure using the adsorption isotherm model, it is known that four models are suitable to describe the adsorption process in the research conducted, namely Jovanic, Freundlich, Halsey, and Dubinin-Rzadushkevich. The correlation coefficient (R^2 = >0.70) was used to determine the validity of this adsorption model. Correlation coefficient values and adsorption parameters are then presented in detail in Table 9.

Figure 3(a) analyses the Langmuir isotherm model which is analysed based on equations (1) and (2). The adsorption data on the Langmuir isotherm model shows the value of R^2 = 0.6899. The maximum adsorption capacity parameter value (Q_{max}) is 121.9512 mg/g. The K_L parameter value is 0.0033 L/mg, and the R_L parameter value is 0.7911-0.9380. This shows that the value of the R_L parameter is in the range of 0 and 1 which informs that the adsorption process is profitable. Based on the value of R^2, it shows the adsorption process belongs to the non-monolayer adsorbent process [31].

Figure 3(b) shows the results of the Freundlich model analysis. The results of the analysis show that the Freundlich model has a value of R^2 = 0.7423 indicating that the adsorption process forms a monolayer. The parameter value of n is 0.8248 indicating the adsorption process that occurs is a chemisorption process because n < 1. The parameter value 1/n has a value of 1.2124 informing that the adsorption process occurs in a cooperative manner [31].

Figure 3(c) shows the results of the Temkin Model analysis which assumes that all molecules on the adsorbent surface have a linearly decreasing heat of adsorption due to uniform energy distribution. Based on the analysis results, the Temkin isotherm model has a value of R^2 = 0.5931 indicating that the adsorption process shows a homogeneous process. Parameter values A_T and β_T were 1.7063 L/g and 0.0993 J/mol, respectively. Based on these parameter values, it provides information that the absorption process occurs physically (Physisorption) [31].

Figure 3(d) shows the results of the calculation analysis of the Dubinin-Raduskevich isotherm model. The Dubinin-Radushkevich isotherm has a value of R^2 = 0.7187 and the value of the E isotherm parameter is 0.3218 kJ/mol indicating that the adsorption process is physically running (E < 8 kJ/mol) [31].

Figure 3(e) shows the results of plotting the analysis of the Fowler Guggenheim isotherm model. The R^2 value of the Fowler Guggenheim model equation is 0.1581 and the W parameter value is 99.1432 kJ/mol. The value of R2 indicates the monolayer adsorption process on the adsorbent surface. Based on the results of the analysis, the value of W > 0 shows there is an attractive force on the adsorbed molecules and the process is exothermic [31].

Figure 3(f) is the result of the analysis curve for the Hill-Deboer. The Hill-Deboer has a value of R^2 = 0.2348 with the parameter value of K_2 being -117.9141 kJ/mol. Based on the K_2 parameter (K_2 < 0 kJ/mol), the adsorption process occurs with interactions between molecules that repel each other, and the adsorption process is a monolayer [31].

Figure 3(g) is the result of plotting data based on the Jovanovic isotherm model. Parameter value R^2 = 0.9379, KJ = 0.1286 L/mg, and Q_{max} is 5.9316 mg/g. The Q_{max} value indicates that Q_{max} value is relatively small, indicating that the adsorbent has a weak adsorption capacity [31]. Based on the R^2 value in the Javanovis isotherm model, the adsorption process that occurs is a monolayer.

Figure 3(h) is the Harkin-Jura adsorption model. The results of the curve analysis of the Harkin-Jura isotherm show that R^2 is 0.3063, from this value it is known that the adsorption process is a monolayer. Harkin-Jura isotherm parameters identified are *AHJ* and *BHJ* parameters with values of 0.0324 and 1.4238, respectively [31].

Figure 3(i) shows the analysis of the Flory-Huggins Model. The correlation coefficient value of this model is R^2 = 0.0466. Based on the value of R^2 shows the adsorption process is a monolayer. n_{FH} parameter values indicate the presence of interactions between free molecules and adsorbed molecules on the adsorbent surface. The interaction occurs because the free molecule attaches and interacts with the adsorbed molecule. The value of Gibbs free energy is also informed by this model. The Gibbs free energy parameter has a negative value which indicates that the adsorption process is spontaneous [31].

Figure 3(j) is the result of Halsey's isotherm analysis. Halsey isotherm shows the value of R^2 = 0.7423 which indicates the adsorption process is a monolayer. Halsey's isotherm constants for K_H and *n* are 86.981 and 0.6601, respectively [31].

An adsorption isotherm is used to find the adsorption model and to define the adsorption process more clearly. Calculations of adsorption models that have been determined previously were carried out to find the value of R^2. The value of R^2 is used to assess the suitability of the adsorption isotherm model. If the value of R^2 is close to 1, then the adsorption isotherm model is more suitable. As for this study, the sequence of adsorption isotherm models that were suitable for removing the colour of curcumin with carbonate from mango seed waste were Jovanovic (R^2 = 0.9379), Freundlich (R^2 = 0.7423), Halsey (R^2 = 0.7423), Dubinin-Radushkevich (R^2 = 0.7187), Langmuir (R^2 = 0.6899), Temkin (R^2 = 0.5931), Harkin-Jura (R^2 = 0.0.3063), Hill-Deboer (R^2 = 0.2348), Fowler-Guggenheim (R^2 = 0.1581), and Flory-Huggins (R^2 = 0.0466). The adsorption results show that four adsorption isotherms are suitable to describe the adsorption process with $R^2 > 0.7$.

Judging from the suitability, the Jovanovic is the most suitable model with the R^2 value closest to 1. By looking at the process of the Jovanovic isotherm model, the adsorption process is a monolayer. However, judging from the overall model that is considered suitable in the experiments carried out by the adsorption process on several adsorption isotherm models, it was concluded that this research is a monolayer adsorption process and the isotherm that occurs in a cooperative manner (confirmed through the Freundlich model). The adsorption process on the adsorbate occurs homogeneously on the adsorbent surface, this is confirmed by the Temkin isotherm model.

Physisorption and chemisorption are the types of interactions that occur. The Freundlich isotherm model confirmed this chemisorption interaction process. Meanwhile, the Dubinin-Radushkevich and Temkin isotherm corroborated the kind of physisorption interaction. Van der Waal's attraction, or weak attraction between molecules, causes physical adsorption [36]. Chemical adsorption, on the other

hand, is the outcome of a stronger force than the creation of chemical compounds [37]. Furthermore, the adsorption process was normal (as validated by the Freundlich isotherm), spontaneous (as shown by the Flory-Huggins isotherm), and favourable in general (confirmed by the Freundlich isotherm).

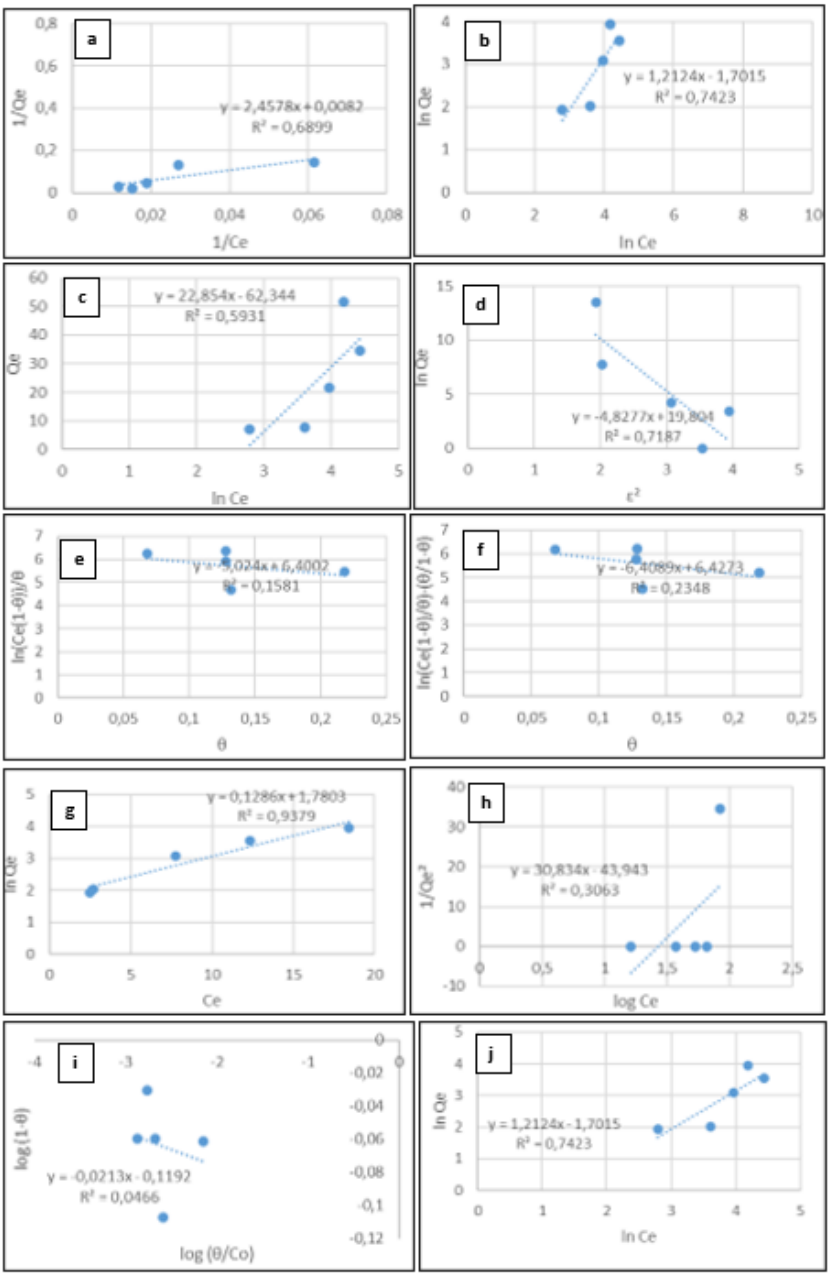

Fig. 3. Data fitting with isotherm models Langmuir: a. Langmuir; b. Freundlich; c. Temkin; d. Dubinin Radushkevich; e. Fowler-Guggenheim; f. Hill-Deboer; g. Jovanovic; h. Harkin-Jura; i. Flory-Huggins; dan j. Halsey.

Table 9. Detailed information on the adsorption isotherm characteristics.

Model	Parameters	Value	Notes
Langmuir	R^2	0.6899	non-monolayer adsorbent process ($R^2 < 0.90$)
	Q_{max} (mg/g)	121.9512	Maximum capacity adsorption
	K_L (L/mg)	0.0033	Small worth The Langmuir constant indicates that there is little interaction between the adsorbate and the adsorbent.
	R_L	0.7911-0.9380	Favourable adsorption ($0 < R_L < 1$)
Freundlich	R^2	0.7423	Monolayer existence on the surface of the adsorbent ($R^2 < 0.90$)
	n	0.8248	chemisorption process ($n < 1$)
	$1/n$	1.2124	Cooperative adsorption process ($1/n < 1$)
	K_f (mg/g)	3.3615	The adsorption capacity of the adsorbent
Temkin	R^2	0.5931	Homogenous adsorbate in the adsorbent surface ($R^2 < 0.90$)
	A_T (L/g)	1.7063	Temkin equilibrium binding constant
	β_T (J/mol)	0.0993	Physisorption ($\beta_T < 8$ kJ/mol)
Dubinin-Radushkevich	R^2	0.7187	The adsorbent surface no contains micropores ($R^2 < 0.90$)
	β (mol^2/kJ^2)	4.8277	Dubinin-Radushkevich isotherm constant
	E (kJ/mol)	0.3218	Physisorption (E < 8 kJ/mol)
Fowler-Guggenheim	R^2	0.1581	Monolayer existence on the surface of the adsorbent ($R^2 < 0.90$)
	W (kJ/mol)	99.1432	The attractive force between the adsorbed molecules and the process is exothermic ($W > 0$ kJ/mol)
	K_{FG} (L/mg)	152.0182	Fowler-Guggenheim isotherm constant
Hill-Deboer	R^2	0.2348	Monolayer existence on the surface of the adsorbent ($R^2 < 0.90$)
	K_1 (L/mg)	0.0016	Hill-Deboer isotherm constant
	K_2 (kJ/mol)	-117.9141	Repulsive interaction between the molecule of adsorbed ($K_2 < 0$ kJ/mol)
Jovanovic	R^2	0.9379	Monolayer existence on the surface of the adsorbent ($R^2 > 0.90$)
	K_J (L/mg)	0.1286	Jovanovic isotherm constant

Model	Parameters	Value	Notes
	Q_{max} (mg/g)	5.9316	maximum absorption of the adsorbate
Harkin-Jura	R^2	0.3063	No multilayer existence on the surface of the adsorbent (R^2 < 0.90)
	A_{HJ}	0.0324	Harkin-Jura isotherm constant
	B_{HJ}	1.4238	Related to the surface area of the adsorbent
Flory-Huggins	R^2	0.0466	Monolayer existence on the surface of the adsorbent (R^2 < 0.90)
	n_{FH}	-0.0213	The adsorbate occupies more than one active adsorbent zone (n_{FH} < 1)
	K_{FH} (L/mg)	1.3158	Flory-Huggins isotherm constant
	$\Delta G°$ (kJ/mol)	2.2218	Spontaneous adsorption ($\Delta G°$ > 0)
Halsey	R^2	0.7423	Monolayer existence on the surface of the adsorbent (R^2 < 0.90)
	n	0.8248	Halsey isotherm constant
	K_H	0.1824	Halsey isotherm constant

5. Conclusion

This research was conducted to conduct an adsorption isotherm experiment on the removal of dye from curcumin solution with mango seed waste carbon microparticles. The batch-reactor technique was used to investigate the adsorption isotherm model. The dye model used is curcumin. The results of this study indicate that several models are suitable for representing adsorption equilibrium with a correlation coefficient close to 1, namely Jovanovic (R^2 = 0.9379), Freundlich (R^2 = 0.7423), Halsey (R^2 = 0.7423), and Dubinin-Radushkevich (R^2 = 0.7187). In general, mango seeds can be used as an adsorbent due to their tannin content as an active substance in the coagulation process and starch as a flocculant. In addition, the bonds between the hydroxyl groups (-OH) of glucose units in adjacent mango seeds in the cellulose molecule can interact with the adsorbate component. Mango seeds have considerable potential to be used as adsorbents. This study shows the potential applications of mango seed waste as a sustainable adsorbent source for carbon microparticles and can support SDGs.

References

1. Azmiyawati, C. (2006). Kajian kinetika adsorpsi Mg (II) pada silika gel termodifikasi gugus sulfonat. *Jurnal Kimia Sains dan Aplikasi*, 9(2), 35-39.
2. Apriyanti, E. (2012). Adsorpsi CO2 menggunakan zeolit: aplikasi pada pemurnian biogas. *Dinamika Sains*, 10(22), 1-11.

3. Jia, X.; Zhang, H.; Zhang, Z.; and An, L. (2019). First-principles investigation of vacancy-defected graphene and Mn-doped graphene towards adsorption of H2S. *Superlattices and Microstructures*, 134, 106235.
4. Kurniasari, L. (2010). Pemanfaatan mikroorganisme dan limbah pertanian sebagai bahan baku biosorben logam berat. *Majalah Ilmiah Momentum*, 6(2), 5-6.
5. Maisuthisakul, P.; and Gordon, M.H. (2014). Characterization and storage stability of the extract of Thai mango (Mangifera indica Linn. Cultivar Chok-Anan) seed kernels. *Journal of Food Science and Technology*, 51(8), 1453-1462.
6. Dorta, E.; Lobo, M.G.; and Gonzalez, M. (2012). Reutilization of mango byproducts: study of the effect of extraction solvent and temperature on their antioxidant properties. *Journal of Food Science*, 77(1), C80-C88.
7. Dhingra, S.; and Kapoor, A.C. (1985). Acceptability of mango seed-kernel flour in conventional food items. *Indian Journal of Agricultural Sciences*, 55(8), 550-552.
8. Poerwanto, D.D.; Hadisantoso, E.P.; and Isnaini, S. (2015). Pemanfaatan biji asam jawa (Tamarindus Indica) sebagai koagulan alami dalam pengolahan limbah cair industri farmasi. *Al-Kimiya: Jurnal Ilmu Kimia dan Terapan*, 2(1), 24-29.
9. Lee, C.S.; Robinson, J.; and Chong, M.F. (2014). A review on application of flocculants in wastewater treatment. *Process safety and environmental protection*, 92(6), 489-508.
10. Mulyani, H.; and Sujarwanta, A. (2017). Kualitas Minyak Jelantah Hasil Pemurnian Menggunakan Variasi Adsorben Ditinjau dari Sifat Kimia Minyak. *Jurnal Teknologi Pangan dan Hasil Pertanian*, 12(2), 19-29.
11. Pérez-Marín, A.B.; Zapata, V.M.; Ortuno, J.F.; Aguilar, M.; Sáez, J.; and Lloréns, M. (2007). Removal of cadmium from aqueous solutions by adsorption onto orange waste. *Journal of Hazardous Materials*, 139(1), 122-131.
12. Hendrasarie, N.; and Pratama, A. (2021). Penurunan kadar krom limbah cair industri penyamakan kulit menggunakan karbon aktif dari limbah kulit sapi dan limbah tumbuhan. *Prosiding ESEC*, 2(1), 81-86.
13. Hayati, U. P.; and Sawir, H. (2017). Pemanfaatan limbah kulit buah kakao sebagai adsorben untuk penyerapan ion logam kromium (vi) pada limbah elektroplating di Bukittinggi. *Jurnal Sains dan Teknologi: Jurnal Keilmuan dan Aplikasi Teknologi Industri*, 17(1), 36-42.
14. Syuhadah, N.; and Rohasliney, H. (2012). Rice husk as biosorbent: a review. *Health and the Environment Journal*, 3(1), 89-95.
15. Adam, D.H. (2017). Kemampuan tandan kosong kelapa sawit sebagai adsorben untuk meregenerasi minyak jelantah. *Jurnal Eduscience* (*Jes*), 4(1), 8-11.
16. Suartini, N.; Jamaluddin, J.; and Ihwan, I. (2018). Pemanfaatan arang aktif kulit buah sukun (artocarpus altilis (parkinson) fosberg) sebagai adsorben dalam perbaikan mutu minyak jelantah. *Kovalen: Jurnal Riset Kimia*, 4(2), 152-165.
17. Juliana, I.N.; Gonggo, S.T.; and Said, I. (2015). Pemanfaatan buah mengkudu (Morinda Citrifolia l.) sebagai adsorben untuk meningkatkan mutu minyak jelantah. *Jurnal Akademika Kimia*, 4(4), 181-188.

18. Imani, A.; Sukwika, T.; and Febrina, L. (2021). Karbon aktif ampas tebu sebagai adsorben penurun kadar besi dan mangan limbah air asam tambang. *Jurnal Teknologi*, 13(1), 33-42.
19. Hanifah, H.N.; Hadisoebroto, G.; Apriani, R.; and Apriani, M. (2020). Efektivitas kulit salak dan biji salak (salacca zalacca) sebagai bioadsorben logam pb dari limbah cair laboratorium farmasi. *Jurnal Sabdariffarma*, 2(2), 13-20.
20. Fiandini, M.; Ragadhita, R.; Nandiyanto, A.B.D.; and Nugraha, W.C. (2020). Adsorption characteristics of submicron porous carbon particles prepared from rice husk. *Journal of Engineering Science and Technology*, 15, 022-031.
21. Nandiyanto, A.B.D.; Hofifah, S.N.; Inayah, H.T.; Putri, S.R.; Apriliani, S.S.; Anggraeni, S.; and Rahmat, A. (2021a). Adsorption isotherm of carbon microparticles prepared from pumpkin (Cucurbita maxima) seeds for dye removal. *Iraqi Journal of Science*, 1404-1414.
22. Nandiyanto, A.B.D.; Girsang, G.C.S.; Maryanti, R.; Ragadhita, R.; Anggraeni, S.; Fauzi, F.M.; Sakinah, P.; Astuti, A.P.; Usdiyana, D.; Fiandi, M.; Dewi, M.W.; and Al-Obaidi, A.S.M. (2020a). Isotherm adsorption characteristics of carbon microparticles prepared from pineapple peel waste. *Communications in Science and Technology*, 5(1), 31-39.
23. Nandiyanto, A.B.D.; Azizah, N.N.; and Rahmadianti, S. (2021b). Isotherm study of banana stem waste adsorbents to reduce the concentration of textile dying waste. *Journal of Engineering Research*, 9, 1-15.
24. Nandiyanto, A.B.D.; Putra, Z.A.; Andika, R.; Bilad, M.R.; Kurniawan, T.; Zulhijah, R.; and Hamidah, I. (2017). Porous activated carbon particles from rice straw waste and their adsorption properties. *Journal of Engineering Science and Technology*, 12(8), 1-11.
25. Ragadhita, R.; Nandiyanto, A.B.D.; Nugraha, W.C.; and Mudzakir, A. (2019). Adsorption isotherm of mesopore-free submicron silica particles from rice husk. *Journal of Engineering Science and Technology*, 14(4), 2052-2062.
26. Nandiyanto, A.B.D.; Arinalhaq, Z.F.; Rahmadianti, S.; Dewi, M.W.; Rizky, Y.P.C.; Maulidina, A.; Anggraeni, S.; Bilad, M.R.; and Yunas, J. (2020). Curcumin adsorption on carbon microparticles: synthesis from soursop (annonamuricata l.) peel waste, adsorption isotherms and thermodynamic and adsorption mechanism. *International Journal of Nanoelectronics and Materials*, 13, 173-192.
27. Nandiyanto, A.B.D.; Maryanti, R.; Fiandini, M.; Ragadhita, R.; Usdiyana, D.; Anggraeni, S.; Arwa, W.R.; and Al-Obaidi, A.S.M. (2020). Synthesis of carbon microparticles from red dragon fruit (Hylocereus undatus) peel waste and their adsorption isotherm characteristics. *Molekul*, 15(3), 199-209.
28. Nandiyanto, A.B.D.; Erlangga, T.M.S.; Mufidah, G.; Anggraeni, S.; Bilad, R.; and Yunas, J. (2020). Adsorption isotherm characteristics of calcium carbonate microparticles obtained from barred fish (scomberomorus spp.) bone using two-parameter multilayer adsorption models. *International Journal of Nanoelectronics and Materials*, 13, 45-57.
29. Huda, T.; and Yulitaningtyas, T.K. (2018). Kajian adsorpsi methylene blue menggunakan selulosa dari alang-alang. *Indonesian Journal of Chemical Analysis* (*IJCA*), 1(1), 9-19.

30. Maryanti, R.; Rahayu, N.I.; Muktiarni, M.; Al Husaeni, D.F.; Hufad, A.; Sunardi, S.; and Nandiyanto, A.B.D. (2022). Sustainable development goals (SDGs) in science education: Definition, literature review, and bibliometric analysis. *Journal of Engineering Science and Technology*, 17, 161-181.
31. Nandiyanto, A.B.D.; Ragadhita, R.; and Yunas, J. (2020). Adsorption isotherm of densed monoclinic tungsten trioxide nanoparticles. *Sains Malaysiana*, 49(12), 2881-2890.
32. Nandiyanto, A.B.D.; Kim, S.G.; Iskandar, F.; and Okuyama, K. (2009). Synthesis of spherical mesoporous silica nanoparticles with nanometer-size controllable pores and outer diameters. *Microporous and Mesoporous Materials*, 120(3), 447-453.
33. Nandiyanto, A.B.D.; Andika, R.; Aziz, M.; and Riza, L.S. (2018). Working volume and milling time on the product size/morphology, product yield, and electricity consumption in the ball-milling process of organic material. *Indonesian Journal of Science and Technology*, 3(2), 82-94.
34. Nandiyanto, A.B.D.; Zaen, R.; and Oktiani, R. (2018). Working volume in high-energy ball-milling process on breakage characteristics and adsorption performance of rice straw ash. *Arabian Journal for Science and Engineering*, 43, 6057-6066.
35. Ragadhita, R.; and Nandiyanto, A.B.D. (2021). How to calculate adsorption isotherms of particles using two-parameter monolayer adsorption models and equations. *Indonesian Journal of Science and Technology*, 6(1), 205-234.
36. Qing, Z.; Qi-Cheng, L.; Peng, L.; Chuan-Sheng, C.; and Jiang-Rong, K. (2020). Study on modification mechanism of nano-ZnO/polymerised styrene butadiene composite-modified asphalt using density functional theory. *Road Materials and Pavement Design*, 21(5), 1426-1438.
37. Meng, F.; Song, M.; Wei, Y.; and Wang, Y. (2019). The contribution of oxygen-containing functional groups to the gas-phase adsorption of volatile organic compounds with different polarities onto lignin-derived activated carbon fibers. *Environmental Science and Pollution Research*, 26(7), 7195-7204.